The Prevalence Of Secondary Cratering Through Analysis Of Recent Impacts On The Moon. K. E. Johnson[1,2] and G. Y. Kramer[2], [1]Rice University, Department of Physics, Houston, TX, [2]Lunar and Planetary Institute, Houston, TX, (johnson@lpi.usra.edu), (kramer@lpi.usra.edu).

Introduction: The purpose of this project is to determine the occurrence and attributes of secondary craters from a single primary crater with limited analytical complications from influences that would alter the surface after the impact event, such as subsequent impact cratering and atmospheric weathering. To do this, we searched for craters who have an incredibly low or complete lack of craters within the crater bowl. Such a lack of craters would be evidence that the crater is recent enough to not have had time to accumulate any subsequent primary impacts and allows us to be confident that any craters we observe on the crater's ejecta blanket are exclusively the secondary craters created when these impacts occurred. The lessons learned from this study could provide valuable information to improve our understanding of the impact cratering process [1] and dating of planetary surfaces using crater size frequency techniques [2, 3, 4]. At the time of writing this abstract, we completed analysis of two lunar craters:

Linné. A 2.4 km diameter crater in west Mare Serenitatis, located at 27.7°N 11.8°E. Linné has a relatively high albedo ejecta blanket compared to the surrounding mare basalts. There are numerous large boulders in the ejecta blanket, with many around 15 to 20 meters in length. One of the prominent features in the ejecta layer of Linné is the unusual rippling pattern in its proximal and extended ejecta blanket.

Eimmart A. A crater on the rim of Eimmart, which is a crater on the rim of Mare Crisium. It is located at 24.1°N and 65.65°E. It is roughly 7.3 km in diameter. Eimmart A is flanked to the west by the wall and edge of Eimmart and to the east by the basalt rock of Mare Crisium.

Despite the plethora of secondary craters observable in both of the craters' continuous ejecta blankets, the crater bowls lack any resolvable impact craters. Secondary impacts would be expected to occur within the perimeter of the transient crater, and during the early stages of modification. However, slumping and collapse of the crater walls would continue long after the return of the ejected material, and thus destroy any evidence of such secondaries.

Data and Methodology: Analysis used data from Lunar Reconnaissance Orbiter's (LRO) Narrow Angle Camera (NAC). Mosaiced images and DEMs were created with USGS Integrated Software for Imager and Spectrometers (ISIS) and NASA Ames Stereo Pipeline (ASP). The horizontal spatial resolution of the Linne NAC mosaic is 0.5 meter/pixel, and the DEM is 2 meters/pixel. The NAC image for Eimmart A has a horizontal resolution of 1 meter/pixel, the DEM is 5 meters/pixel. The Environment for Visualizing Images (ENVI) was used to determine the precise area of the mapped ejecta blanket.

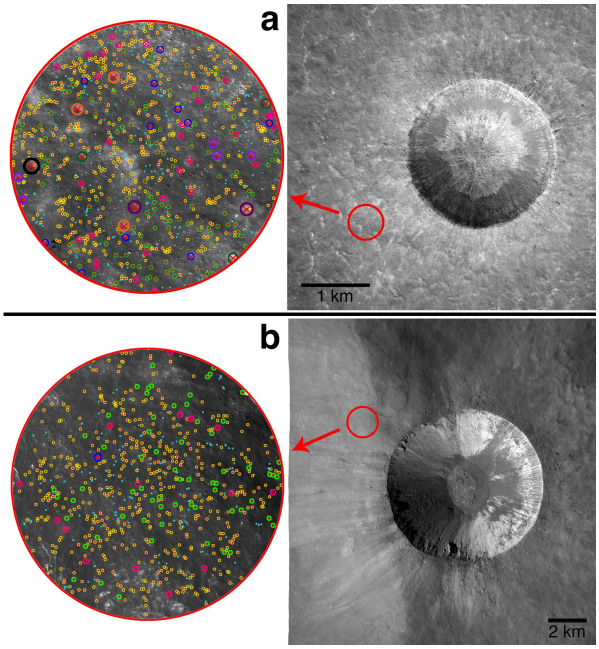

Figure 1: (Right) NAC mosaic of the analyzed primary impact craters, Linne (a) and Eimmart A (b). (Left) Locations of counted secondary impact craters from focus region (with color-coded bin sizes). Red circle on ejecta blanket identifies the location of the focus region.

Each crater's ejecta blanket was mapped out to ~1 crater diameter from the rim. The specific boundary was based on a combination of the DEM and on morphology. For quantitive analysis, a circle with a diameter of 3 crater radii was centered on the crater. This circle was divided into 8 equal pie-slice sections. A circle containing the crater bowl and subtracted from each 8 sections makes up a 9th section. For each section we mapped easily recognized craters, which all turned out to be >12x the resolution of the NAC mosaic. This was done to evaluate the uniformity of secondary crater density around the primary crater and ensure that the selection of the focus region would be representative of the region. No craters were observed in the 9th section (bowl) of either crater.

A circle of diameter = 1000 pixels was selected for detailed analysis from approximately midway between the crater rim and perimeter of the continuous ejecta

blanket and that had a representative secondary crater density (Fig. 1). Every resolvable crater within this circle was counted and binned by size, where each bin represented a range of 4 pixels (Fig. 1).

Results: For both studied craters, the binned crater counts show the distribution curve expected for a standard particle size distribution, with the exception of the smallest bin size. We calculated an expected crater size frequency for the smallest bin size using the midpoint diameter for each bin. Tables 1 and 2 show the results for Linné and Eimmart A, respectively, of the binned craters counted from the representative region, the modeled count for the smallest bin, and the values extrapolated for the entire continuous ejecta blanket. Figure 2 shows the plot of the curves.

Conclusion: We attribute the deviation of the smallest bin size from the expected distribution to because the size range is too close to the spatial resolution of the data set. We do not believe the deviation of the first bin reflects a lower limit to the size of secondary craters created [e.g., 5] or that survive the debris surge [e.g., 6] from a primary impact for two reasons: 1) the distribution of particle sizes in crater ejecta is expected to increase asymptotically with decreasing grain size, and 2) if there was such a limit, we would expect to see the curve turn over at some point when looking at smaller bin size. The results from Linné do not show such a downturn despite having much better spatial resolution (both absolutely and proportionally) than Eimmart A. Instead, the count increases with decreasing bin size, until the smallest bin size, suggesting the apparent downturn is a consequence of data resolution.

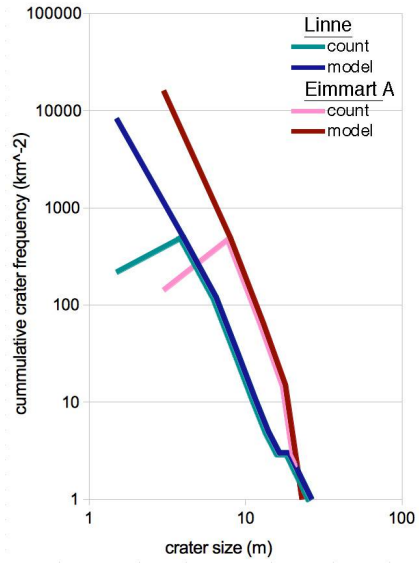

Figure 2: Frequency size distributions for secondary craters counted on the continuous ejecta blankets of Linne and Eimmart A.

Interestingly, despite the evidence that virtually all craters counted at Linné and Eimmart A are their respective secondaries, the individual craters exhibited varying grades of apparent degradation, that is, some rims having prominent crests, while others being very subdued. We assume this reflects difference in time between formation, albeit on a severely limited period of time. That the more subdued craters landed early and were partly covered by fine particle debris, while the more prominent secondary craters landed later. However, we recognize that this hypothesis contradicts what is understood about ballistic trajectories of impact rater ejecta.

We were surprised to find almost 10^6 secondary impact craters that could be resolved in orbital remote sensing data from LRO NAC for these simple lunar craters. In addition, the observed variations in crater morphology, that would typically be attributed to degradation by resurfacing over time, may explain apparent inconsistencies in models that use crater size frequency distributions. Although these secondaries are very small impact craters, our instruments are improving our ability to observe them and making it increasingly difficult to ignore them. The results from this study has specific relevance for calculations meant to adjust crater counting results to account for secondaries counted as part of a surface dating analysis.

Acknowledgments: Buck Sharpton for generating the mosaic and DEM of Linné, and Teemu Öhman for generating the mosaic and DEM of Eimmart A.

References: [1] Melosh, J. H. *Impact Cratering: A Geologic Process* (1989). [2] Neukum, G. et al. (1975) *The Moon 12*: p. 201-229. [3] Hartmann, W.K. et al. (1981) *BVSP*, p. 1049-1127. [4] Stöffler, D. & Ryder, G. (2001) *Space Sci. Rev. 96*. [5] Allen, C. (1979) *GRL 6*. [5] Wilhelms, D. E. et al. (1978) *Proc. LPSC 9th*. [7] Kirchoff, M. E. (2013) *Icarus 225*.

Table 1: Results for Linne

bin	count	modeled	extrapolated	error
0.5-2.5m	217	8280	***794880***	2496
3-5 m	503	503	***49728***	2208
5.5-7.5 m	120	120	9888	1056
8-10 m	31	31	3168	576
10.5-12.5 m	11	11	1344	384
13-15 m	5	5	672	288
15.5-17.5 m	3	3	384	192
18-20 m	3	3	288	192
20.5-22.5 m	2	2	192	192
23-25 m	0	0	96	96
25.5-27.5 m	1	1	96	96

Table 2: Results for Eimmart A

bin	count	modeled	extrapolated	error
1-5m	142	16000	***944000***	1416
6-10m	493	493	***29500***	1298
11-15m	65	65	3894	472
16-20m	15	15	944	236
21-25m	1	1	295	59